A multi-criteria decision support framework for designing seismic and thermal resilient facades

Kim, Kyujin; Luna-Navarro, Alessandra; Ciurlanti, Jonathan; Bianchi, Simona

DOI
10.1007/s44150-024-00116-0

Publication date
2024

Document Version
Final published version

Published in
Architecture, Structures and Construction

Citation (APA)
Kim, K., Luna-Navarro, A., Ciurlanti, J., & Bianchi, S. (2024). A multi-criteria decision support framework for designing seismic and thermal resilient facades. *Architecture, Structures and Construction*, *4*(2-4), 195-210. https://doi.org/10.1007/s44150-024-00116-0

Architecture, Structures and Construction (2024) 4:195–210
https://doi.org/10.1007/s44150-024-00116-0

RESEARCH

A multi-criteria decision support framework for designing seismic and thermal resilient facades

Kyujin Kim[1] · Alessandra Luna-Navarro[1] · Jonathan Ciurlanti[2] · Simona Bianchi[1]

Received: 23 February 2024 / Accepted: 12 September 2024 / Published online: 30 September 2024

Abstract
Facades play a pivotal role in the performance of a building, serving various environmental, structural and operational functions. As climate-induced extreme events become more frequent, developing resilient facades is becoming crucial. Although facades can contribute significantly to the total post-disruption losses, their resilience is not sufficiently addressed in current design approaches. In response to this research gap, this study proposes a multi-criteria decision-making methodology to select optimal facade designs using resilience criteria: resilience loss and economic loss. The framework addresses the complexity of facade design, considering multiple hazards such as earthquakes and heatwaves. For seismic hazard, the facade's resilience is defined as its ability to mitigate damage. In the case of heat hazard, resilience is assessed based on the ability to keep indoor conditions within a comfortable thermal range. To demonstrate the applicability of the proposed methodology, a case study of an 18-story office building in Izmir (Turkey) is used to compare alternative facade packages. These packages identify the facade design cases, each coupled with a dataset of seismic and thermal fragility curves. Numerical simulations are conducted to derive seismic and thermal resilience curves for each facade package, along with resilience criteria. These criteria are embedded into a practical decision-making process to enable the selection of the optimal design case based on project specifications.

Keywords Resilient facade · Multi-criteria decision making · Seismic resilience loss · Thermal resilience loss · Fragility curve

Introduction

The growing discourse on resilience in the built environment is largely due to increasing frequency and intensity of external environmental hazards imposed by climate change. The concept of resilience has emerged from a shift in focus, moving from prevention of climate change to preparation for and acceptance of its inevitable uncertainties. The National Academy of Sciences defines resilience as 'the ability to prepare and plan for, absorb, recover from, and more successfully adapt to adverse events' [1]. Thus, the resilience of a system can be engineered by implementing predictive risk assessment and mitigation strategies for focused disturbances. The facade, which lies between a building's exterior and interior, performs a variety of complex functions, including environmental, structural, and operational aspects. Enhancing the resilience of the facade not only pertains to these functions, but it's also related to the overall resilience of the building. Patterson et al. [2] discuss the scalability of resilience, arguing that focusing on defining specific resilience characteristics of a facade system can improve not only the resilience of the facade itself but also the overall resilience of the larger built environment.

Despite its potential impact on the resilience of the built environment, facade resilience is not sufficiently addressed. Facade components are classified as non-structural elements in the current earthquake design code [3]. While these elements are significantly vulnerable to disruptive events, they are not yet adequately designed to withstand earthquakes

✉ Kyujin Kim
K.J.Kim@tudelft.nl

✉ Alessandra Luna-Navarro
A.LunaNavarro@tudelft.nl

Jonathan Ciurlanti
Jonathan.Ciurlanti@arup.com

Simona Bianchi
S.Bianchi@tudelft.nl

[1] Delft University of Technology, Julianalaan 134, Delft 2628 BL, The Netherlands

[2] Arup Amsterdam, Naritaweg 118, Amsterdam 1043 CA, The Netherlands

[4]. The design of the building envelope plays a significant role in enhancing thermal resilience, especially for passive habitability during long power outages that coincide with extreme weather events (e.g., extreme cold or hot conditions) [5]. These design strategies encompass thermal insulation, air barriers, fenestration, window-to-wall ratio, shading devices, natural ventilation, and thermal mass. When dealing with severe and prolonged heatwaves, implementing all these passive measures has proven effective in maintaining the upper habitability threshold.

There is limited research on multi-hazard resilience assessment and design, and particularly in facade engineering. The recent Façade Resilience Evaluation Framework, introduced by Favoino et al. [6], has provided a qualitative evaluation tool that assesses risks associated with specific facade designs within varying geographical and social contexts. It also identifies measures and mitigation strategies for reducing such risks in a climate change scenario. The study found that implementing resilience reviews early in the design process can have a greater impact and reduce mitigation costs. However, in order to directly compare design choices and quantify potential improvements of implementing a specific design strategy, a quantitative approach is needed. Attia et al. [7] conducted a literature review on the qualitative performance of cooling technologies during extreme events and concluded that a quantitative approach is necessary for directly comparing technologies in future studies. A multi-hazard approach is essential for defining resilience and addressing the diverse challenges faced by building facades. The city resilience framework [8] demonstrates that the recent concept of resilience has moved from traditional disaster risk management, focused on specific hazards, to enhancing performance against multiple hazards. The principle of Facade Resilience [2] underscores the necessity for building designs capable of anticipating future uncertainty, thus adaptable to diverse circumstances, rather than solely focusing on specific weather conditions.

The main hazards associated with facades include earthquakes, blast, wind, and heat. In the field of facade engineering, these hazards are seen as exceptional loads applied to the facade. Design regulations provide minimum acceptable standards. According to Eurocode 8 [3], nonstructural components should be designed to provide adequate clearance gaps which accommodate the relative horizontal displacements of the primary load-bearing structure. In US FEMA 450 [9], specific inter-story drift values are provided for ‘glazed curtain walls’, ‘storefronts’, and ‘partitions’ . Blast requirements for facade components are outlined in UFC 4-010-01 [10], which aims to ensure dynamic material strength . Research on improving facade design to reduce the impact of various hazards includes: improving seismic performance of facade systems [4], enhancing blast resistance of glazing curtain walls [11], assessing wind risk for cladding and glazing [12], and mitigating heat stress risk with phase change materials [13]. In the typical approach to designing facades to withstand multiple hazards, the process is divided by load case, with each member and connection sized individually for each case. As a result, any synergies or conflicts between cases can be overlooked, leading to unnecessary design iterations [14]. Design decisions made for one performance area can impact another, creating a trade-off in hazard resistance. To avoid this, a multi-hazard approach should be incorporated into the facade design process. Unlike when only a single hazard is considered, this approach involves making holistic design decisions that meet multiple design requirements.

In summary, the current facade design procedure does not ensure multi-hazard resilience, despite the significant damage to the facades caused by various hazards. This is due to the absence of a methodology where facade selection decisions are based on resilience criteria. This issue is compounded by the fact that hazard intensity indices and indicators for assessing the impact of disruptive events vary across studies, and there is no established combined resilience metric. To address this, this study proposes a practical multi-criteria decision-making process for facade design. The methodology has two main objectives: (i) to offer a quantitative assessment procedure for evaluating facade systems’ resilience to multiple hazards (earthquakes and heatwaves), and (ii) to establish a workflow for choosing among alternatives based on multi-criteria indicators of facade systems’ resilience performance.

The paper is structured as follows: Section “Multi-criteria decision making for facades resilient to seismic and heat hazards” introduces the proposed multi-criteria decision-making methodology. Section “Case study” describes the settings of the case study where this methodology is tested. Section “Results” presents the results of the case study and the results are discussed in Section “Discussion”. Finally, Section “Conclusion” concludes by reflecting on the applicability of the methodology.

Multi-criteria decision making for facades resilient to seismic and heat hazards

Incorporating resilience into decision-making involves identifying criteria that help distinguish between different facade design options. This study proposes a novel decision-support framework which evaluates various facade design options based on two criteria: resilience loss and economic loss. The resilience of a system is mathematically characterized by the time variation of functionality, representing the system’s response and recovery to a disruptive event. The resilience loss can be measured by the integral of expected degradation in quality ($Q(t)$) over time, as defined by Bruneau [15], with

the following formula:

$$\text{Resilience Loss} = \int_{t_0}^{t_1} [1 - \text{Q(t)}]\text{dt} \quad (1)$$

Here, t_0 represents the start of the facade function degradation following a disruptive event, and t_1 indicates the time when the full resilience of the facade components is restored. The resilience index (ranging between 0 and 1, where 1 means no resilience loss) is determined by the integral of the functionality function over a specific time period [15]. According to this definition, resilience is enhanced by minimizing the loss of resilience. Another decision-making criterion is the economic aspect. This involves measuring the economic loss by assessing the cost of enhancing resilience. Enhancing or engineering resilience means improving the system's ability to withstand a certain demand and quickly recover to its previous state. As a result, the costs associated with these enhancements are taken into account.

This framework adopts a multi-hazard approach, with a focus on earthquakes and extreme heat. Each hazard is considered to occur independently and is therefore defined separately. As discussed in the "Introduction" section, hazards can affect various aspects of facade functionality. The impact of an earthquake on a facade's functionality can be determined by the extent of damage to the facade components at a specific inter-story drift. The more severe the damage, the more repairs are required. The damage factor, which is the ratio of repair cost to replacement cost, is used to define the quality function:

$$Q(t) = 1 - \frac{RepairCost}{ReplaceCost} \quad (2)$$

Equation 2 indicates that when no facade repair costs are needed, the functionality $Q(t)$ is at its maximum, represented by 1. Yet, if the repair cost equals the replacement cost, the functionality drops to 0. This indicates that repair is no longer viable, making it more practical to replace the entire building. The quality function allows for the generation of a functionality curve, which includes both functionality drop, downtime, and recovery through repair. Downtime is the overall time needed to achieve re-occupancy or restore functionality [16]. It includes the delay between the earthquake event and the start of repairs. In Section A4.3 of REDi report [16], a methodology for assessing this overall business interruption is presented, which provides an overview of the downtime calculation. Finally, the seismic resilience loss is calculated using Eq. 1, incorporating the quality function from Eq. 2. Economic loss is defined as the cost incurred in repairing the damaged components.

The impact of extreme heat on a facade's functionality - its ability to maintain indoor conditions within the thermal comfort range without the need for mechanical cooling, a concept known as passive survivability or thermal autonomy - is evaluated by occupants' discomfort, not physical damage. Occupant discomfort is measured by the standard effective temperature (SET), which takes into account six factors: air temperature, radiation temperature, relative humidity, air velocity, metabolic rate, and clothing insulation. This index combines meteorological and physiological parameters, effectively illustrating the interaction between the human body and its environment. It's assumed that the facade's functionality is at 1 within the comfort SET threshold, and decreases to 0 beyond the alert SET threshold. The mathematical formulation of the quality function in this research was adapted from an assessment of indoor environment quality by Bucking et al. [17]:

$$Q(t) = \begin{cases} 1 & \text{if } SET(t) \leq SET_{comf} \\ 0 & \text{if } SET(t) \geq SET_{alert} \\ \frac{SET_{alert} - SET(t)}{SET_{alert} - SET_{comf}} & \text{otherwise} \end{cases} \quad (3)$$

If the standard effective temperature $SET(t)$ exceeds SET_{alert} = 32°C, it's considered a failure, with a quality function of 0. If $SET(t)$ is below SET_{comf} = 24°C, it falls within the comfort range, with a quality function of 1. The quality function linearly interpolates the SET between 24°C and 32°C. Finally, the thermal resilience loss, which indicates the degree hours above the thermal comfort threshold during a heatwave, is calculated using Eq. 1. This incorporates the quality function from Eq. 3. The economic loss is estimated by the cost of the cooling energy that would have been needed to mitigate the effect of a heatwave.

Figure 1 illustrates the proposed multi-criteria decision-making approach's workflow. The process begins with defining design alternatives for multi-criteria evaluation; each alternative is a facade package that includes seismic and thermal fragility specifications. Following this, a performance assessment of these alternatives is conducted. Earthquake hazards are defined using a response spectrum, while heatwave hazards are represented through weather data. The impact of these hazards on the facade is evaluated using a numerical model simulating structural behavior under seismic demand, and an analytical model simulating thermal and energy performance during heatwaves. Resilience criteria, such as resilience loss and economic loss, are measured through performance evaluation and loss modeling. These criteria are utilized to select a facade alternative. This choice can be made by either weighting the criteria or not, depending on the specific requirements of the project.

Table 1 offers definitions for the metrics and indicators used in this research to assess seismic and thermal resilience.

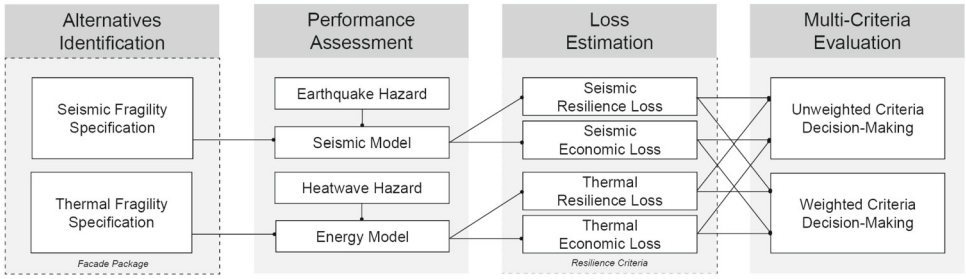

Fig. 1 The decision-support framework for selecting seismic and thermal resilient facades involves identifying alternatives, assessing performance, estimating losses, and conducting multi-criteria evaluation

Formulate facade alternatives by combining seismic and thermal fragility datasets

A facade package is used to represent a facade alternative for multi-criteria resilience assessment. Table 2 describes a facade package configuration. This package is a data set that includes both seismic and thermal fragility specifications, with each specification containing one for an opaque wall and one for a window. The seismic fragility data is sourced from the FEMA P-58 fragility database or literature findings, as discussed below. In total, four opaque and four glazing seismic fragility curves were utilized. Packages A01-B01, C01-D01, A02-B02, and C02-D02 all have the same specification. The thermal fragility data is generated by running a dynamic thermal simulation in EnergyPlus and using a maximum likelihood fitting procedure [18] to create the fragility function. In total, four opaque and two glazing fragility curves were used. Packages A01-C01, B01-D01, A02-C02, and B02-D02 have the same specification for opaque. Packages A01-B01-C01-D01 and A02-B02-C02-D02 share the same specification for glazing.

Seismic fragility specifications

FEMA P-58 Volume 3 [19] includes a fragility database with over 700 individual fragility specifications. This database

Table 1 Definitions of indicators for evaluating seismic and thermal resilience

Indicators	Earthquake	Heatwave
Representation	Response spectrum of peak ground acceleration with 10% probability of exceedance in 50 years	Weather data with heatwave events, defined as daily maximum temperature exceeding 5°C for five consecutive days
Fragility curve	Probability of reaching or exceeding damage state, given demand parameter	Probability of reaching or exceeding thermal comfort threshold, given demand parameter
Intensity measure	Peak ground acceleration	Temperature anomaly
Demand parameter	Inter-story drift	Outdoor air temperature
Functionality curve	Functionality drop at a disruptive event, followed by a period of downtime and recovery	Temporary functionality reduction and recovery throughout the disruptive event
Functionality drop	Damage of component characterized in discrete damage states	Proportional deviation of standard effective temperature from the thermal comfort threshold
Recovery	Repair of damaged components	Standard effective temperature nearing the thermal comfort threshold
Resilience loss	Severity of damage expressed by the ratio of repair cost to replacement cost	Degree hours above the thermal comfort threshold during a heatwave
Economic loss	Total repair cost of components	Estimated cooling energy cost incurred during a heatwave

Table 2 Seismic and thermal fragility specifications of facade packages (IGU - insulated glass unit)

	Seismic fragility specifications		Thermal fragility specifications	
	Opaque	Glazing	Opaque	Glazing
A01	B2011.121	B2022.201	W0.05T01	W0.95T01
	Wood frame	Unitized curtainwall	Composite wall	Double pane
	Sheet panel	IGU	concrete, insulation	Low-E, clear glass
B01	B2011.121	B2022.201	W0.05C01	W0.95T01
	Wood frame	Unitized curtainwall	Mass wall	Double pane
	Sheet panel	IGU	concrete, concrete	Low-E, clear glass
C01	B2011.302a	B2022.011	W0.05T01	W0.95T01
	Concrete cladding	Curtain wall	Composite wall	Double pane
	U-shaped plate	Asymmetric IGU	concrete, insulation	Low-E, clear glass
D01	B2011.302a	B2022.011	W0.05C01	W0.95T01
	Concrete cladding	Curtain wall	Mass wall	Double pane
	U-shaped plate	Asymmetric IGU	concrete, concrete	Low-E, clear glass
A02	B2011.301	B2023.002	W0.05T02	W0.95T02
	Masonry infill	Storefront	Composite wall	Double pane
	French window	IGU	concrete, insulation	Planibel, clear glass
B02	B2011.301	B2023.002	W0.05C02	W0.95T02
	Masonry infill	Storefront	Mass wall	Double pane
	French window	IGU	concrete, concrete	Planibel, clear glass
C02	B2011.302	B2022.091	W0.05T02	W0.95T02
	Concrete cladding	Curtain wall	Composite wall	Double pane
	Tie-back connection	Symmetric IGU	concrete, insulation	Planibel, clear glass
D02	B2011.302	B2022.091	W0.05C02	W0.95T02
	Concrete cladding	Curtain wall	Mass wall	Double pane
	Tie-back connection	Symmetric IGU	concrete, concrete	Planibel, clear glass

contains extensive data on curtain wall cladding, but lacks information for facade materials like masonry and concrete. The specifications for these materials were derived from the following sources: Fragility specifications for concrete panels with U-shaped flexural plate connections (B2011.302a) and tie-back connections (B2011.302) were obtained from Bianchi and Pampanin [20], who derived the data from the test reports of Baird et al. [21]. Information on masonry infill walls (B2011.301) was sourced from Cardone et al. [22].

Thermal fragility specifications

Current frameworks for assessing heat vulnerability and thermal resilience often do not incorporate the concept of fragility and its probabilistic nature, focusing more on immediate impacts of heat exposure. However, there have been attempts to include fragility in these assessments. In a study by Szagri and Szalay [23], fragility curves were used to evaluate heat vulnerability. These curves evaluated the conditional probability of overheating during heatwave periods by examining the probability of exceeding indoor temperature given outdoor temperature. Fragility curves were generated using a maximum likelihood method developed by Baker [18], which is a fitting procedure used to determine the parameters of a distribution (fragility function) that are most likely to generate the observed data. For this research, maximum likelihood fitting is applied in the same manner, with the difference being that the mean outdoor temperature is used as the intensity measure, and the standard effective temperature (SET) is used to define the limit state.

A shoebox model, representing a typical inter-story floor configuration for the case study, is used to calculate fragility functions for various components. The analysis uses typical meteorological year (TMY) weather data, recording the SET temperature of one of the four parameter zones on the south-facing side, throughout the year.

Table 3 shows the facade construction layers for each of the thermal fragility specifications; four for the fully opaque facade and two for the fully glazed facade. Each specification is formulated to represent a facade component with different thermal properties such as thermal transmittance (U-value), specific heat capacity, and solar heat gain coefficient (SHGC). For the fully opaque wall, the window-to-wall ratio is set at 0.05. A composite wall made of concrete and thick insulation (W0.05T01) has a U-value of 0.5W/m^{2}K, while a wall with thinner insulation (W0.05T02) has a U-

Table 3 Facade construction layers for thermal fragility specifications

Facade package	Fragility ID	Thermal property	Layer 1	Layer 2	Layer 3	Layer 4
A01, C01	W0.05T01	U:0.49	Stucco	Concrete	Insulation	Gypsum
		C:428	t:0.0253	t:0.2032	R:1.76	t:0.0127
A02, C02	W0.05T02	U:2.24	Stucco	Concrete	Insulation	Gypsum
		C:428	t:0.0253	t:0.2032	R:0.7	t:0.0127
B01, D01	W0.05C01	U:1.12	Stucco	Concrete	Concrete	Gypsum
		C:1950	t:0.0253	t:0.0826	t:0.6096	t:0.0127
B02, D02	W0.05C02	U:2.35	Stucco	Concrete	Concrete	Gypsum
		C:808	t:0.0253	t:0.2032	t:0.2032	t:0.0127
A01, B01,	W0.95T01	U:2.36	Low-E	Air Gap	Clear Glass	
C01, D01		G:0.42	t:0.006	t:0.0127	t:0.006	
A02, B02,	W0.95T02	U:2.37	Planibel	Air Gap	Clear Glass	
C02, D02		G:0.54	t:0.006	t:0.0127	t:0.006	

Layer 1 represents the exterior facing layer and Layer 4 represents the interior facing layer (U - thermal transmittance; R - thermal resistance; C - specific heat capacity; G - solar heat gain coefficient; t - thickness)

value of 2.3W/m^{2}K. A mono-material wall made of thick concrete (W0.05C01) has a heat capacity of 1950J/K, while a thinner concrete wall (W0.05C02) has a heat capacity of 808J/K. For the fully glazed wall, the window-to-wall ratio is set at 0.95. An insulated glazing unit of Low-E coated glass (W0.95T01) has an SHGC value of 0.42, while Planibel Clealite, a glass product from AGC with high light transmission, has an SHGC value of 0.54.

Fragility functions are created for three limit states (LS1=24°C, LS2=28°C, LS3=32°C) using daily mean outdoor air temperature as the intensity measure. The objective of the fragility analysis is to determine the probability of the indoor thermal environment exceeding the limit state at a given outdoor air temperature. This can be formulated as follows:

$$P(\text{SET} \geq \text{threshold} \mid IM = x_j)_{observed} = \frac{\text{number of hours when } IM = x_j}{\text{number of hours per day}} \tag{4}$$

The probability of SET reaching the limit state threshold, given the intensity level x_j is represented by P. This probability can be expressed as the number of hours in a day during which SET exceeds the limit state, divided by the total number of hours in the day. Based on the observed probabilities, a fragility curve, assuming a lognormal cumulative distribution function, is then fitted using the maximum likelihood method.

Derive resilience criteria through loss estimation

The general procedure for probabilistic loss assessment, as shown in Fig. 2, estimates potential resilience loss based on the probability of a hazard occurrence and specific fragility parameters. The fragility curves enable to calculate the probability of achieving or exceeding different damage limit states (DS). Information on the damage and its consequential loss for each limit state is combined to establish vulnerability. Alongside the recovery scenario (e.g. post-earthquake repairing actions), a functionality curve is created and the total loss is finally calculated. When evaluating the resilience of facade packages, this procedure is adapted for each seismic and thermal loss assessment.

Seismic loss assessment is conducted using the FEMA P-58 methodology [19] and its Performance Assessment Calculation Tool (PACT) [24]. A seismic-resistant numerical building model is constructed and analyzed via linear static analysis with OpenSeesPy [25]. The post-earthquake losses of the building are calculated using PACT, which provides estimates for repair costs, repair times, casualties, and environmental impacts. The resulting output can be processed and filtered based on performance groups and number of floors. While the repair of both structural and nonstructural components of a building may be interconnected, this analysis specifically focuses on the resilience and economic loss of the facade component, which falls under the nonstructural component category.

The evaluation process for thermal loss shares a similar approach to the FEMA P-58 methodology. However, due to the absence of an established fragility curve or loss modeling protocol, this paper proposes a unique method for creating these elements. Fragility curves are developed using the SET index, illustrating the probability of reaching or exceeding a SET threshold at a specified outdoor air temperature. The building energy model is created using Honeybee [26], and dynamic thermal simulations in EnergyPlus [27] are used to analyze the building's response. Both resilience and eco-

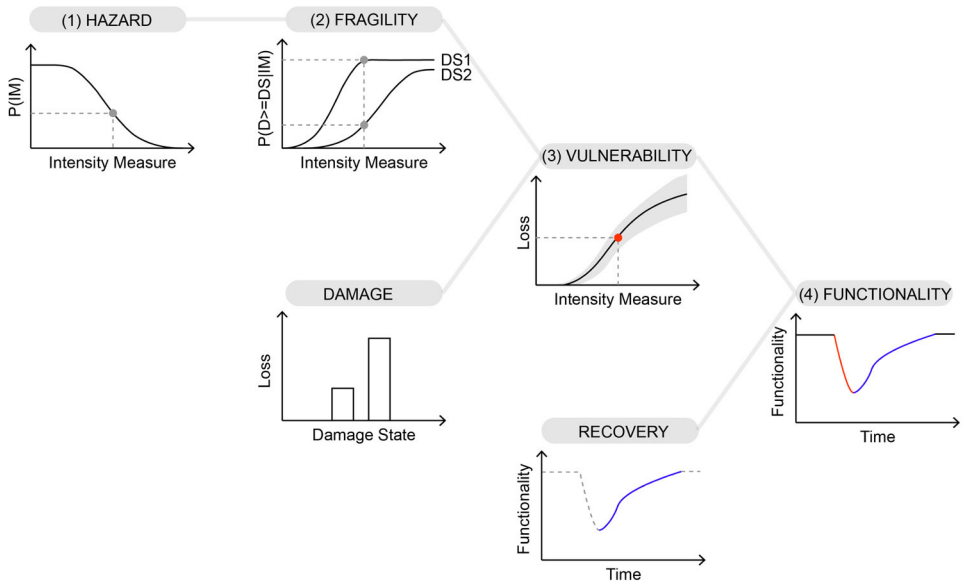

Fig. 2 The procedure for probabilistic loss assessment includes: (1) probability of a hazard occurring at a given intensity, (2) probability of reaching or exceeding a damage limit state at a given intensity, (3) probability of reaching or exceeding loss consequences at a given intensity, and (4) quality function of functional drop and recovery over time

nomic loss are calculated from the EnergyPlus SQL output, which helps form a functionality curve that includes both the drop and recovery in functionality. The functionality drop is viewed as a proportional deviation of SET from the thermal comfort threshold. Recovery is defined as the SET approaching the thermal comfort threshold.

Select design options based on multi-criteria analysis

The combined score for each alternative is calculated by multiplying each criterion by its respective weight, and finally summing these weighted values. The alternative with the smaller combined score ranks higher. The combined score for each alternative is given by:

$$\text{Score}_i = w_1 \cdot \text{SRL}_i + w_2 \cdot \text{SEL}_i + w_3 \cdot \text{TRL}_i + w_4 \cdot \text{TEL}_i$$

where Score_i is the combined score for the i-th alternative. SRL_i, SEL_i, TRL_i, and TEL_i are the seismic resilience loss, seismic economic loss, thermal resilience loss, and thermal economic loss for the i-th alternative, respectively. The weights w_1, w_2, w_3, and w_4 are assigned to these criteria. The weights are determined by project specifications and user needs, including factors such as hazard exposure and the building's intended use.

Case study

To validate the methodology outlined in Section "Multi-criteria decision making for facades resilient to seismic and heat hazards", a case study was considered. This study focuses on an 18-story office building in Izmir, Turkey. Izmir was chosen due to its medium to high risks associated with seismic and heat hazards. As shown in Fig. 3, the building has a square floor plan, measuring 22.5m on each side, with each story being 3m high. The structure comprises reinforced concrete (RC) frames and RC shear walls. The centrally located shear walls are flanked by columns situated along the building's perimeter, separating the structural elements from the facade. The window-to-wall ratio is 0.5. On each floor, half of the total 270m^2 facade surface is allocated to the opaque wall and the other half to the window. Both the opaque and window walls span the full story height. For uniformity in all perimeter zones, the facade alternates between opaque and window sections in a stripe pattern.

Seismic performance of case study building

Earthquake - response spectrum

Peak ground acceleration (PGA), with a 10% probability of exceedance in 50 years, was chosen as the seismic hazard for the case study. This is equivalent to a return period of 475 years. Data for the response spectrum of the 2013 European Seismic Hazard Model (ESHM13) was obtained from the EFEHR web platform [28]. This platform provides seismic hazard data that can be accessed by selecting a specific site location and hazard model.

Figure 4 shows a plot of the response spectrum, with the fundamental period of vibration (T=1.56s) for the case study building indicated. The fundamental period of vibration is the point at which the structure experiences the most significant vibrations when exposed to dynamic loading. Factors such

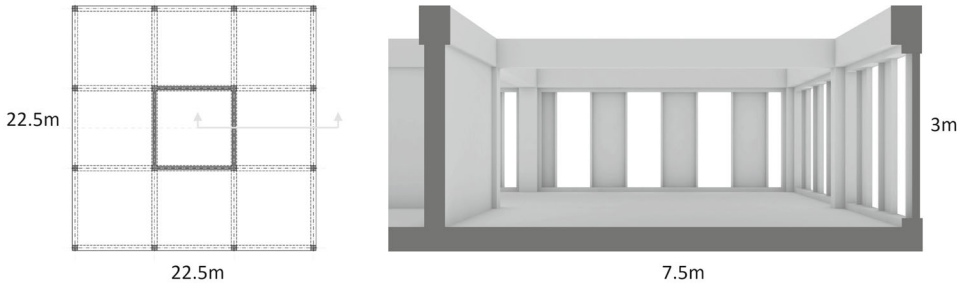

Fig. 3 Illustration of the case study building structural framework (floor plan) and facade design, with a 0.5 window-to-wall ratio in the perimeter zones (perspective)

as the building's mass, stiffness, and geometry influence its definition though modal analysis.

Seismic model

The structural design of the RC dual system was carried out by referencing ASCE/SEI 7-16, "Minimum Design Loads and Associated Criteria for Buildings and Other Structures" [29]. This document suggests minimum safety-related seismic performance criteria for various structural systems. The structural system utilized in this research falls under Category B.5 Building frame systems, specifically Ordinary Reinforced Concrete Shear Walls. The lateral resisting systems were designed considering a mass of 736 tons per floor, based on research by Ciurlanti et al. [30] where the structural type and area dimensions match this building's design.

A finite element model of the multi-story, multi-bay frame structure built with reinforced concrete cross-section elements was created using OpenSeesPy. The structure consists of two bays, with columns located on the outer line and shear walls on the central line. Both the beam and column elements have a uniform cross-section measuring 500 mm x 500 mm, with 30mm diameter rebars within the section. The shear wall is simplified as a cluster of columns. Both the reinforced concrete (RC) frame and the wall were modeled using Force beam-column elements from the OpenSees library. The concrete part of the RC structure used the Concrete02 uniaxial model, with a compressive strength of 28 MPa. The reinforcement part used the Steel02 uniaxial model, with a yield strength of 420 MPa. The integration of the element section was based on Lobatto integration. A linear transformation was used for the beam element in a geometric transformation, while a P-Delta transformation was used for the column and wall elements.

A linear static analysis was carried out using the equivalent lateral force method. This method simplifies the incorporation of inelastic dynamic response effects into a linear static analysis. However, it is only applicable when the primary response to ground movements is in the horizontal direction, with minimal torsion. The process first entails determining the seismic base shear and then distributing this shear force along the height of the structure. Figure 5 illustrates the procedure for applying distributed lateral loads, measuring displacement per floor, and calculating the induced inter-story drift ratio per floor.

The seismic response coefficient of the structure (C_s=0.027) was determined from the design spectral acceleration (S_a = 0.14g). Given the effective seismic weight (W=131035 kN), the seismic base shear (V = 3550 kN) was calculated. The inter-story drift was computed from the nodal displacement in the Fx direction after the lateral load was applied. The inter-story drift ratio θ, the relative horizontal displacement

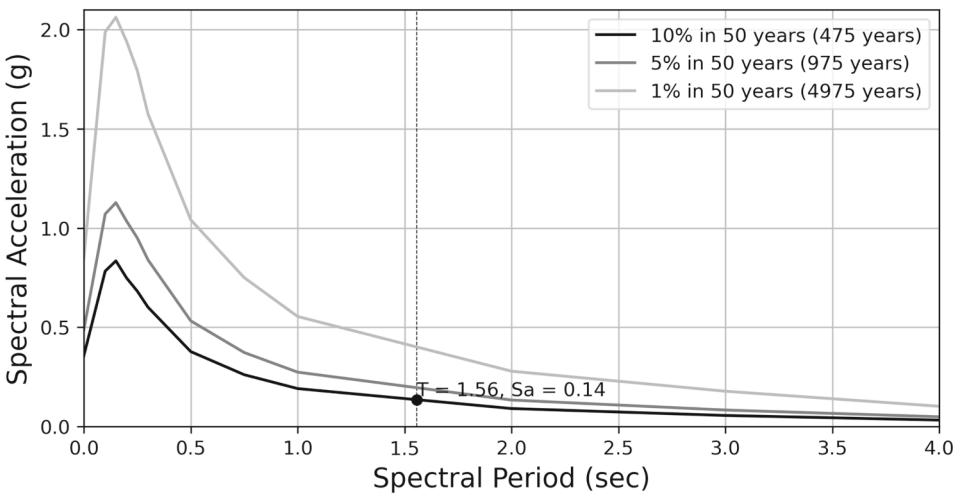

Fig. 4 The response spectrum for a return period of 475 years indicates a spectral acceleration (S_a = 0.14g) at the fundamental vibration period (T = 1.56 seconds)

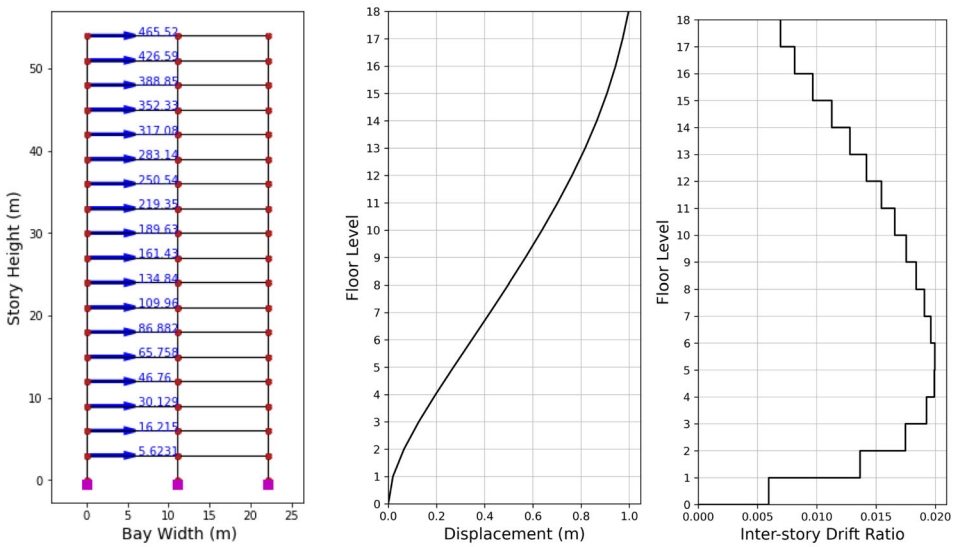

Fig. 5 Equivalent lateral force procedure and inter-story drift calculation

(a) Load Distribution (b) Floor Displacement (c) Inter-story Drift Ratio

between two consecutive floors, is defined as follows:

$$\theta_i = \frac{\delta_i - \delta_{i-1}}{h_i - h_{i-1}} \tag{5}$$

Here, $\delta_i - \delta_{i-1}$ is the change in displacement at floor level i, while $h_i - h_{i-1}$ represents the story height of floor level i. After the inter-story drift ratio is obtained, it is adjusted for inelastic behavior and higher modes effects using the FEMA P-58 Volume 1 Equation 5-10 [19]. The correction factor for each story is assigned based on the first mode of period and the total building height.

Thermal performance of case study building

Heatwave - weather data

The World Meteorological Organization (WMO) defines a heatwave as a period when the daily maximum temperature exceeds the normal maximum by 5 degrees celsius for more than five consecutive days. The normal period is defined as 1961-1990. Recent studies have focused on heatwave detection models and examined specific driving factors in different regions [31]. A method proposed by Flores et al. [32] uses Ouzeau's model to detect heatwaves and assess their impact on the indoor environment. Ouzeau's model characterizes heatwaves by duration (number of days), intensity (maximum mean daily temperature), and severity (mean daily temperature above a threshold). The degree of indoor overheating is used to classify heatwaves based on their impact on indoor environments.

There are currently no internationally agreed-upon protocols for heatwaves, as detection models differ across regions. This paper used a quasi heatwave detection procedure, which involved finding a recorded heatwave from the literature and then applying the WMO's heatwave definition to determine its specific period.

Turkey experienced its most intense heatwave in May 2020, the most severe since 1950. Daily air temperatures in May 2020 exceeded 100-year return periods at many stations across Turkey [33]. Most available weather files, typically based on typical meteorological year (TMY) data, do not account for abnormal events like heatwaves. Consequently, the actual meteorological year (AMY) for Izmir in 2020 was used. The AMY data for Izmir in 2020, obtained from Solcast [34], was converted into an EPW file for use. To pinpoint the exact heatwave period within 2020, a comparison between TMY and AMY data was conducted. This comparison identified the time period where the daily maximum temperature of TMY data exceeded AMY data by more than 5°C for five consecutive days. For TMY data, the file TUR-IZ-Izmir-Adnan.Menderes.Univ.172190-TMYx was used, covering the period 1989-2021. As seen in Fig. 6, the heatwave periods were May 12th to 18th and December 25th to 30th. The most significant daily maximum temperature difference during the heatwave period was 13°C on May 15th.

Energy model

As shown in Fig. 7, the thermal zone was divided into a core and four perimeter zones, each with a depth of five meters, as per the guidelines from ASHRAE Standard 90.1 [35]. This research used an open plan layout, setting the inter-zone wall to have a U-value of 3.24W/m^{2}K and the boundary condition between floors as adiabatic. A 'MediumOffice Building' was chosen from the Honeybee Building Program library.

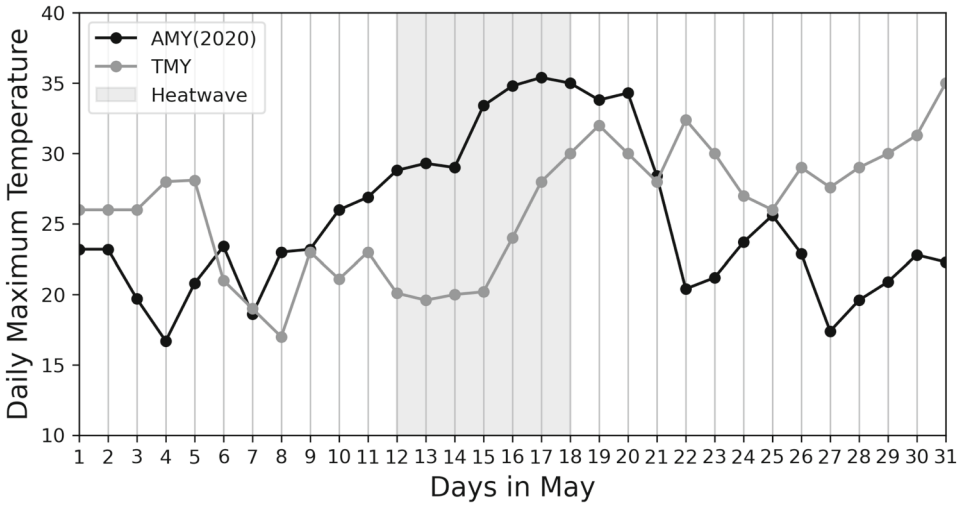

Fig. 6 Typical Meteorological Year (TMY) and Actual Meteorological Year (AMY) for Izmir in May

The program for medium office buildings includes the preset values and schedules for the simulation, as described in Table 4.

The purpose of the energy simulation was to assess the facade components' effectiveness in maintaining comfort during a heatwave, thus excluding other SET influencing factors. The cooling system was turned off during the heatwave and operated at a limited capacity outside the heatwave period to avoid pre-heatwave overheating. To apply these settings in EnergyPlus, the energy simulation was performed in two scenarios.

The first model, calculated the cooling capacity, using the design day (DDY) file from the TMY weather data. This model represents a realistic system where the sizing is based on typical weather conditions, not extreme events like heatwaves. For instance, in Zone 2, the maximum total cooling capacity for the Ideal Loads Air System Design was 11,442W. 70% of this maximum capacity, or 8,009W, was set as the cooling capacity limit for the second model.

The second model, which had a cooling capacity limit, allowed for mechanical cooling operations except during the heatwave period. However, even without cooling operations, mechanical ventilation was set to continue operating during the heatwave, primarily to release internal heat at night rather than following the occupancy schedule. Nighttime ventilation helps cool the system and stabilize the building's thermal condition daily. This strategy proved effective in preventing the SET from surpassing the outdoor temperature due to overheating when cooling was unavailable.

In addition to the energy simulation for measuring SET, a separate simulation ran in parallel to calculate economic losses. In this simulation, the cooling system was also set to operate during the heatwave. The cooling energy consumption/cost during the heatwave was then used as the hypothetical cost that would have been incurred to compensate for the loss of thermal comfort associated with a specific facade type.

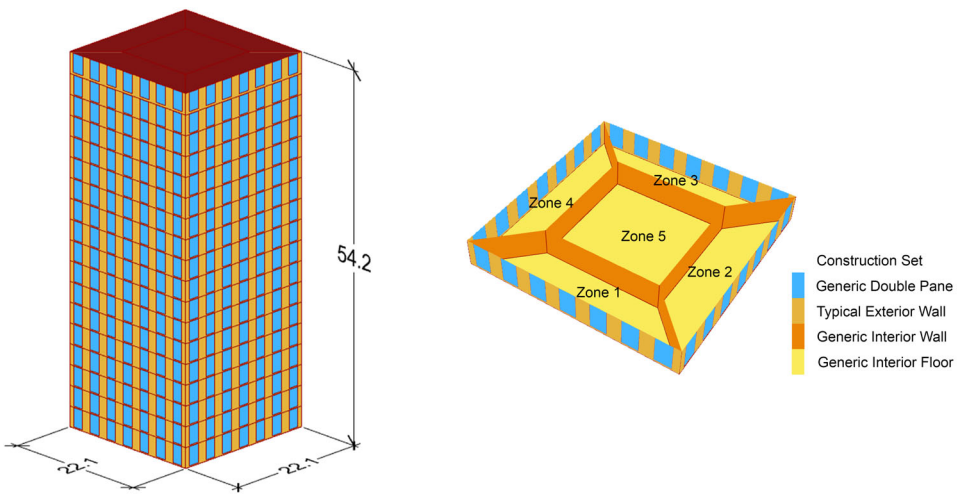

Fig. 7 Illustration of the energy model of an 18-story office building, with the thermal zones of a typical floor (Zone 2 - South facing)

Table 4 Input parameters and settings of energy models used for simulating thermal performance during a heatwave

Energy model	Parameter	Values
Common values	Simulated area	Zone 2 - South facaing
	Occupancy	0.071 people/m^2
	HVAC system	Ideal loads air system
	Setpoint	Heating 21°C, Cooling 24°C
Model 1	Calculate cooling capacity limit based on typical weather conditions	
	Weather data	Typical meteorological year data
	Design day	78 design days
Model 2	Measure standard effective temperature during heatwave	
	Weather data	Historical heatwave data
	Cooling operation	Cooling turned off only during the heatwave
	Cooling capacity limit	70% of maximum capacity of Model 1
	Ventilation	ACH 3
Model 3	Calculate energy consumption and cost during heatwave	
	Weather data	Historical heatwave data
	Cooling operation	Continuous cooling
	Cooling capacity limit	70% of maximum capacity of Model 1
	Ventilation	ACH 3

Results

Fragility curves of facade packages

Figure 8 presents the fragility curves of eight facade packages. Figure 8(a) depicts the seismic fragility curves for four opaque and four glazing facades. Among the three damage states (slight, light, and heavy), the heavy damage state is shown. This includes the fracture of studs and steel plate cracking (opaque, facade packages A01, B01), corner cracking and sliding of mortar joints (opaque, facade packages A02, B02), and glass fall out (glazing, all facade packages). Figure 8(b) shows the thermal fragility curves for four opaque and two glazing facades. Of the three limit states (LS1=24°C, LS2=28°C, LS3=32°C), the limit state of 32°C is presented for comparison. It was not possible to find a different fragility parameter from the initial guess parameter of mean 0.8 and standard deviation 0.5 for the other two limit states. The difficulties in identifying the fragility parameters could be due to insufficient data or the suitability of the fragility model.

For seismic fragility curves of facade packages, the intersection is marked when the demand parameter, the inter-storey drift ratio, reaches 2%. This value is the allowable drift limit according to ASCE 7-10 [29]. When comparing the opaque wall, the wooden stud wall (package A01, B01) has a 15% lower probability of reaching damage state 1 than the masonry infill (package A02, B02). When comparing the glazing wall, the unitized curtain wall (package A01, B01) has a 27% higher probability of reaching limit state 1 than the Storefront (package A02, B02).

For thermal fragility curves, the intersection points represent the probability of reaching the limit state when the intensity measure, which is the mean outdoor temperature, is 28°C. This is the temperature threshold for a heatwave, as defined by the Met Office [36]. When comparing different wall types, the composite wall with high insulation (packages A01 and C01) has a 21% lower probability of reaching limit state 3 than a composite wall with low insulation (packages A02 and C02). Also, when comparing different glazing types, double-pane glazing with a high shading effect (packages A01 and C01) has a 1% lower probability of reaching limit state 3 than double-pane glazing with a low shading effect (packages A02 and C02).

Resilience loss and economic loss of facade packages

Seismic loss estimation

Using the PACT intensity-based results, the repair cost for each floor of each performance group was calculated. The mean repair cost per floor out of 200 realizations was then determined. The total repair cost per floor for the facade components B2011.301and B2023.002 was defined as the sum of their individual repair costs. The total replacement cost was determined as a proportion of the facade replacement cost out of building replacement. For a unitized system that covers the entire building envelope, the estimated cost is 20-30% of the total building cost according to existing literature [37]. From the previously defined replacement cost of the whole building, which is €2,029,714, €608,914 (30%) was defined as the total replacement cost of the facade components. Based

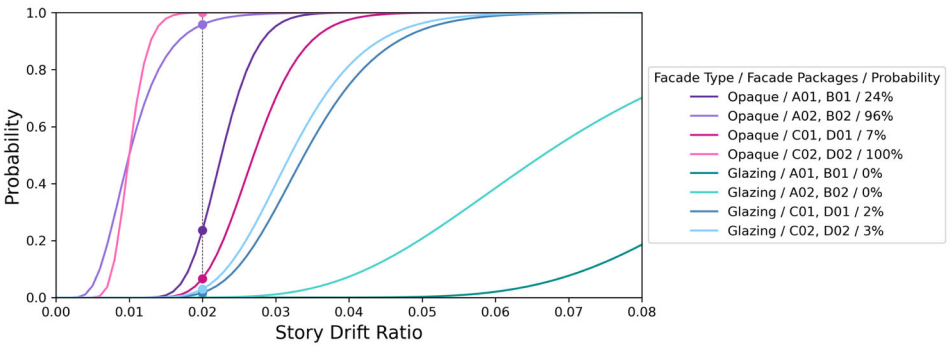

(a) The seismic fragility curve shows the probability of reaching or exceeding heavy damage state, given the story drift ratio

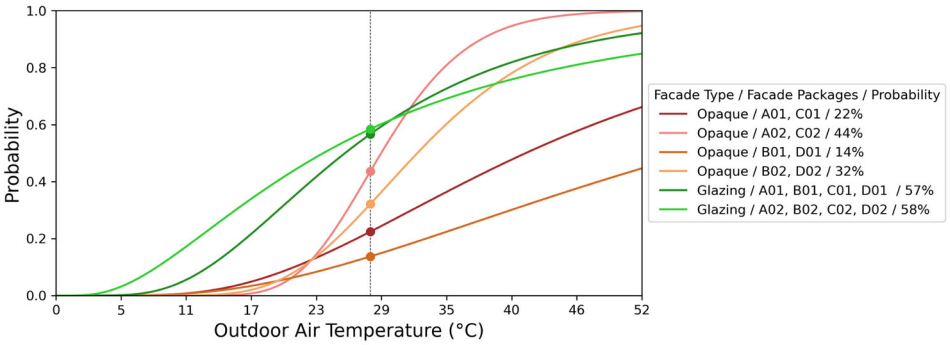

(b) The thermal fragility curve shows the probability that the standard effective temperature will reach or exceed 32°C, given the outdoor air temperature

Fig. 8 Seismic and thermal fragility curves of facade packages

on the repair cost per floor and the total replacement cost, the extent of the functionality drop is quantified.

As depicted in Fig. 9(a), the functionality curve is a function of time. It divides into three sections: impeding factors that delays the initiation of repairs, structural repair time, and facade repair time. These sections represent the time period from the earthquake's onset to the system's complete recovery. As the earthquake occurs, functionality decreases from 100% to 84%. During the structural repair time, the facade functionality is entirely lost. During the facade repair time, there is a proportional drop of functionality per floor of the facade. The total resilience loss results in 112 days of functionality.

The total downtime for this project was calculated by combining the delay time, structural repairs, and facade repairs. A median delay time of 35 weeks (246 days) was used, accounting for factors such as engineering mobilization and review, financing, contractor mobilization, and permitting.

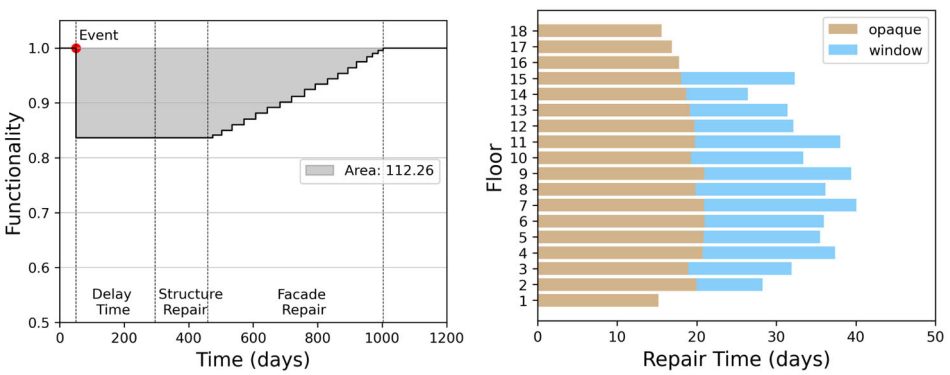

(a) Seismic Functionality Curve (b) Repair Time for Opaque and Window

Fig. 9 Seismic loss estimation of package A02 and package B02 (masonry infill wall with storefront glazing)

Structural repairs were planned concurrently, with the repair time for the floor requiring the most work considered as the total repair time for the entire structure. On the other hand, facade repairs were scheduled sequentially, correlating repair time per floor with the recovery of functionality for that floor. The repair time for each floor is shown in Fig. 9(b). This process results in incremental steps in the functionality curve. These steps indicate that as each floor is repaired and the repair time has passed, the functionality of that floor is restored to its previous level. The repair process for this facade package took a total of 543 days.

Thermal loss estimation

Figure 10(a) shows the SET during heatwave for the two scenairos. Figure 10(b) displays the functionality curve during a heatwave. The thermal functionality curve indicates that, without any repairs, the system naturally recovers over time. This is primarily due to the outdoor air temperature fluctuations. As the temperature falls at night, the SET temperature decreases as well, restoring the functionality drop. The resilience loss is evaluated using a quality function, as per (1) used for measuring seismic resilience loss.

The economic loss was calculated by comparing the cooling energy consumption of two energy models - one operating during a heatwave and the other not. It was assumed that mechanical cooling could reduce the functionality drop by bringing the SET closer to the thermal comfort threshold. The theoretical cooling consumption and its cost were calculated to estimate the resources needed to return to a neutral state. For 10th floor, the model with cooling operation consumed 312.50 kWh of total cooling energy, costing €78.90 at an electricity tariff of 0.2525 €/kWh. The model without cooling consumed 261.37 kWh, costing €65.99. The difference in cost, €12.91, represents the final economic loss.

The resilience and economic losses were calculated for three representative floors: the bottom, the top, and the middle 10th floor. The resilience loss, measured in degree-hours, was 67.30 for the first floor, 81.81 for the 10th floor, and 78.05 for the 18th floor. The loss cost, in Euros, was 20.42 for the first floor, 12.9 for the 10th floor, and 16.87 for the 18th floor. Summing up the losses from the representative floors, the total loss was 227.20 degree-hours and 50.20 Euros. The results indicate that the middle floor experiences the most substantial resilience loss, despite incurring the lowest economic loss. It may seem logical to assume that more degree hours of discomfort would lead to higher cooling energy consumption and increased energy costs. However, the cooling system's efficiency causes more energy consumption when the cooling load is small but frequent, compared to when the load is large but infrequent.

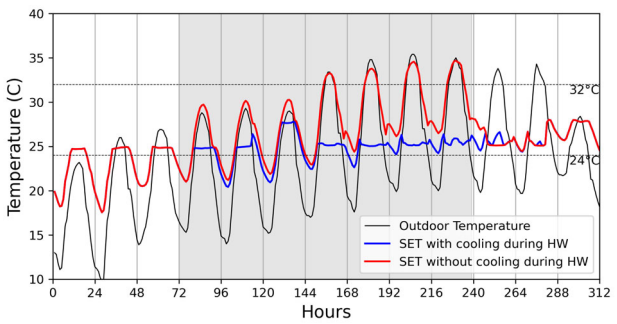

(a) Standard Effective Temperature during Heatwave

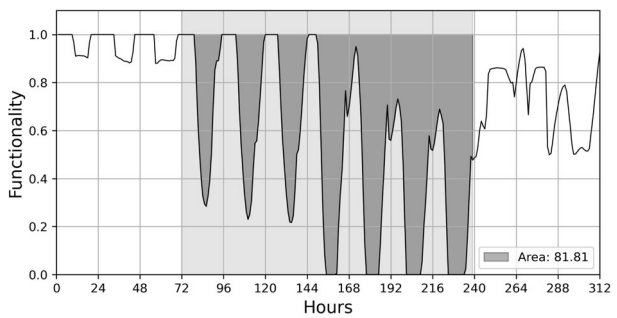

(b) Thermal Functionality Curve during Heatwave

Fig. 10 Thermal loss estimation of package A01 and package C01 (composite wall with double-pane glazing)

Multi-criteria evaluation

The multi-criteria evaluation results for the facade packages are presented in Fig. 11. The results are measured in terms of resilience criteria, specifically resilience loss and economic loss. Each seismic and heat hazard is assessed with two criteria, with a total of four criteria used for decision making. A radar chart presents the values of various criteria for each facade package. Each criterion on the radar chart has been reparameterized to a scale from 0 to 1 based on their own maximum and minimum values. This adjustment allows different units and scales to be visually compared on the same chart. The filled-in area of the radar chart represents the overall resilience characteristics of each facade package. This area value is computed using real values from the adjacent table. A smaller area value corresponds to lower losses in resilience and economics, indicating greater overall resilience.

Facade packages are evaluated using unweighted decision criteria, treating all decision factors as equally important. This method simplifies the comparison of facade packages based on the smallest total resilience loss. It is particularly useful for quickly identifying the most appropriate facade type for a project during the initial design stages. Among the eight packages, package B01 - which includes a wood frame with a concrete mass panel and a unitized curtain wall with

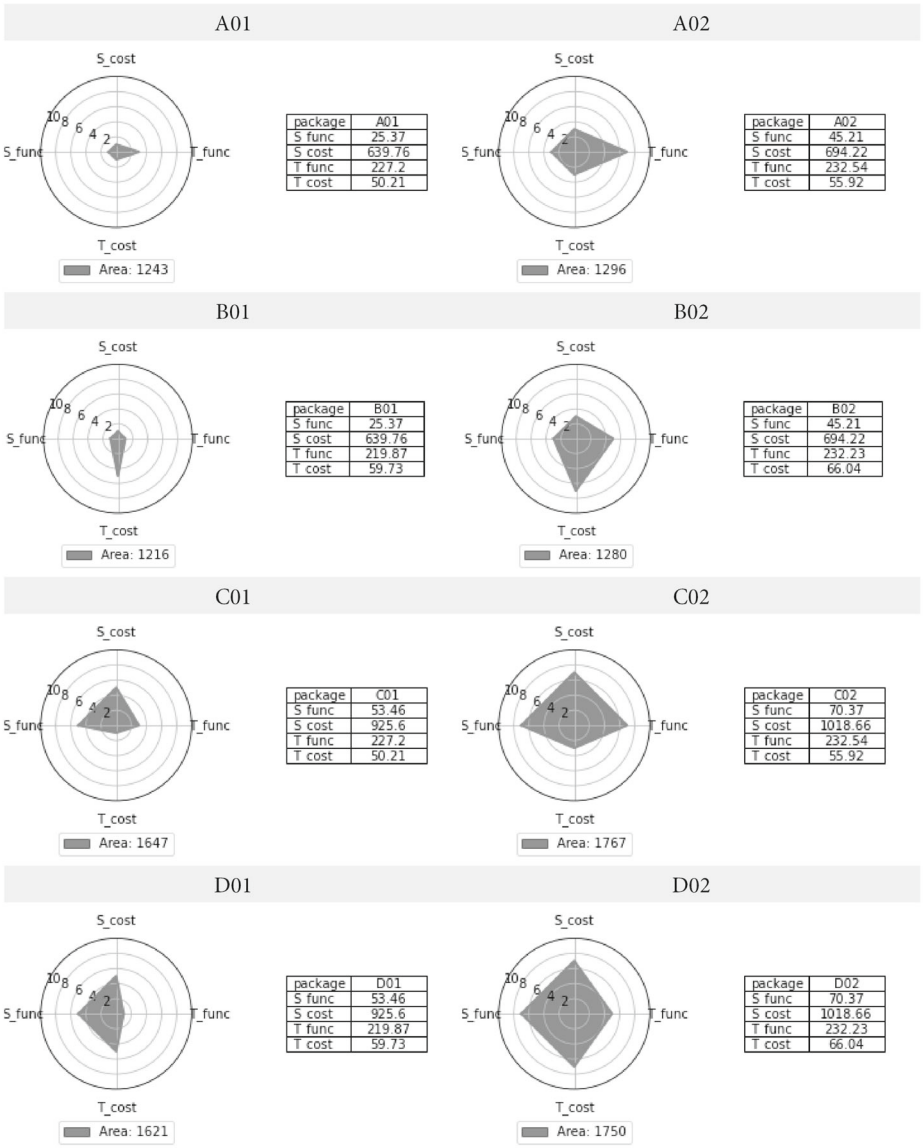

Fig. 11 Multi-criteria evaluation of facade packages (S_func - seismic resilience loss; S_cost - Seismic economic loss; T_func - thermal resilience loss; T_cost - thermal economic loss)

double pane glazing - was ranked as the most resilient facade option. In contrast, package C02 - a concrete cladding system with a tie-back connection, a low-mass concrete panel, and a stick curtain wall system with low-performing double pane glazing - was deemed the least resilient facade option.

Weighting decision criteria become important when additional factors are considered. Rather than comparing based on the combined resilience loss, weights are assigned to specific criteria. For instance, a project may prioritize a facade option resistant to heat hazard over seismic hazard. Although package C01 has a larger combined loss than package B02, assigning more weight to thermal resilience and economic loss criteria may lead to the selection of package C01. The purpose of the building is another key consideration. A hospital, for example, would prioritize minimizing thermal resilience loss over cost, as indoor comfort is essential. If 'thermal resilience loss' is assigned more weight, despite its higher cost, package B02 might be the preferred choice over A02.

Discussion

A facade package, which includes seismic and thermal fragility curves, was used to represent the characteristics of a facade design case in extreme events. By combining different seismic and thermal fragility levels, alternatives were created for comparing facade packages. This allowed for informed decision-making regarding the resistance of a specific facade design to both seismic and heat hazards. However, since the study compares the alternatives in terms of fragility curves,

the number and type of facade options depend on the available fragility curves.

A multi-criteria evaluation of various facade packages revealed that those with a low probability of reaching or exceeding a set threshold result in less resilience loss. This was evident when comparing seismic resilience loss between the unitized curtain wall and storefront system, and thermal resilience loss between highly insulated and less insulated facade composite walls. This research used the limit values provided by the design code to compare fragility curves. However, it should be noted that the level of fragility and the resulting loss can vary based on the standard used for comparison.

Besides resilience loss, economic loss was also factored into the multi-criteria for decision making. This included the estimated repair cost for seismic hazards and the recovery cost to reach a habitable threshold with mechanical cooling under heat hazard. These costs give a projected expense for restoring functionality to its original state.

While loss estimation can be beneficial for decision-making, it is important to understand that this study primarily supports early-stage decisions. Therefore, the accuracy of the loss estimation must be critically reviewed. For seismic performance evaluation, an existing database was used where each seismic fragility curve is linked to repair data. This allowed the estimation of losses for various facade design cases using the inter-story drift ratio derived from a single building structural analysis. However, simplified methods were used in the performance assessment. A linear static approach was applied to assess a high-rise building's resistance, and downtime was estimated by assigning a fixed period for delay time and structural repair time. For thermal performance evaluation, mechanical cooling was turned off exclusively during the heatwave. This was done to assess the facade's contribution to heatwave resilience, while eliminating any prior influence. The resilience of the facade was then assessed using the standard effective temperature as a habitability threshold, in relation to the outdoor air temperature. The correlation between these two factors was formulated into a fragility curve. However, it is important to note that the current formulation of thermal fragility curves may not accurately represent a specific facade composition, as it is based on a single historical heatwave event and a specific thermal zone size.

Conclusion

This paper introduces a practical methodology for making facade design decisions based on multiple resilience criteria. A quantitative assessment procedure was used to evaluate the resilience of a facade design case to earthquake and heatwave hazards. The methodology was validated through a case study of an 18-story office building in Izmir (Turkey). The key findings from this multi-criteria decision-making approach for resilient facade selection are as follows:

- Resilience-related criteria such as seismic/thermal resilience loss and economic loss are crucial variables for addressing design decision processes, which provide a weighted assessment tailored to specific project constraints.
- The introduction of the "facade package" concept aids in formulating alternatives for multi-criteria evaluations. This package encompasses seismic and thermal fragility specifications, enabling a systematic assessment of the effectiveness of facade typologies in building resilience.
- The identification of resilience key indicators enable the evaluation of the hazards' impact on facade performance. This addresses a gap in current facade engineering: the lack of a methodology that considers the risk of multiple extreme hazard scenarios.

For future applications, several improvements to the methodology and calculations should be considered. Firstly, the development of a fully probabilistic-based workflow that includes joint probabilities of multiple hazards and vulnerability should be a priority. This approach would also necessitate identifying the impact indicator at the facade level, thus moving beyond a building-level assessment. In this context, a sensitivity analysis might be used to identify the most relevant indicator, such as demand parameters or resilience loss, which can accurately represent the impact of a heatwave on facade performance. Identifying suitable fragility fitting methods for thermal specifications and developing thermal fragility functions should also form part of this process.

Acknowledgements Not applicable

Author Contributions K.K. contributed to conceptualization, methodology, formal analysis, data curation, visualization, and drafted the original manuscript. A.L.-N. contributed to conceptualization, methodology, supervision, and review. J.C. contributed to supervision and review. S.B. contributed to conceptualization, methodology, supervision, review and final draft editing.

Funding This study has received funding from the European Union under the Horizon Europe Research & Innovation Programme (Grant Agreement no. 101123467 MultiCare).

Availability of Data and Materials The data that support the findings of this study are available on request from the corresponding author, K.K.

Declarations

Competing Interests The authors declare no competing interests.

Ethical Approval Not applicable

References

1. National Research Council (2012) The Nation's Agenda for Disaster Resilience. Disaster Resilience: A National Imperative, pp 1–244. https://doi.org/10.17226/13457
2. Patterson M, Kensek K, Noble D (2017) Supple skins: considering the relevance. Scalability, and Design Strategies for Façade System Resilience. 71(1):34–45. https://doi.org/10.1080/10464883.2017.1260919
3. European Comitee for Standardisation (1998) EN 1998-1:2004/AC:2009 - Eurocode 8: Design of structures for earthquake resistance - Part 1: General rules, seismic actions and rules for buildings. Brussels, Belgium. https://standards.iteh.ai/catalog/standards/cen/b72212d1-f818-46ed-8d30-86442dc67cf1/en-1998-1-2004-ac-2009
4. Baird A et al (2011) Focusing on reducing the earthquake damage to facade systems. Bulletin of the New Zealand Society for Earthquake Engineering 44(2):108–120. https://doi.org/10.5459/bnzsee.44.2.108-120
5. Kesik T, Liam O (2019) Thermal Resilience Design Guide Thermal Resilience Design Guide Graphic Design. Tech. rep
6. Favoino F, Chalumeau A, Aquaronne A (2022) Facade Resilience Evaluation Framework: A Qualitative Evaluation Tool To Support Resilient Facade Design Decision Making. Facade Tectonics 2022 World Congress
7. Attia S et al (2021) Resilient cooling of buildings to protect against heat waves and power outages: key concepts and definition. Energy Buildings 239:110869. https://doi.org/10.1016/J.ENBUILD.2021.110869
8. The Rockefeller Foundation and Arup (2014) City Resilience Index. Tech. rep, Understanding and measuring city resilience
9. Building Seismic Safety Council (2003) FEMA 450:2003. https://www.bssconline.org
10. US Department of Defense (2018) United Facilities Criteria (UFC) DoD Minimum Antiterrorism Standards for Buildings. Tech. rep
11. Bedon C, Amadio C (2018) Numerical assessment of vibration control systems for multi-hazard design and mitigation of glass curtain walls. J Build Eng 15:1–13. https://doi.org/10.1016/J.JOBE.2017.11.004
12. Beers PE (2011) Wind Risk Assessments for Cladding and Glazing in Critical Facilities
13. Ramakrishnan S et al (2017) Thermal performance of buildings integrated with phase change materials to reduce heat stress risks during extreme heatwave events. Appl Energy 194:410–421. https://doi.org/10.1016/J.APENERGY.2016.04.084
14. Mckay AE et al (2015) Multi-Hazard Design of Facades: Important Considerations of Wind and Seismic Interaction with Blast Requirements. Tech. rep
15. Bruneau M, Reinhorn A (2006) Overview of the Resilience Concept
16. Almufti I, Willford M (2013) REDi ™ Rating System Resilience-based Earthquake Design Initiative for the Next Generation of Buildings. Tech. rep
17. Bucking S et al (2022) On modelling of resiliency events using building performance simulation: a multi-objective approach. J Building Performance Simulation 15(3):307–322. https://doi.org/10.1080/19401493.2022.2044906
18. Baker JW (2015). Efficient Analytical Fragility Function Fitting Using Dynamic Structural Analysis. https://doi.org/10.1193/021113EQS025M
19. Applied Technology Council (2018) FEMA P-58-1, Seismic Performance Assessment of Buildings, vol 1 - Methodology, Second Edition. https://femap58.atcouncil.org/reports
20. Bianchi S, Pampanin S (2022) Fragility functions for architectural nonstructural components. J Struct Eng 148(10). https://doi.org/10.1061/(ASCE)ST.1943-541X.0003352
21. Baird A, Palermo A, Pampanin S (2013) Controlling Seismic Response using Passive Energy Dissipating Cladding Connections. 2013 NZSEE Conference
22. Cardone D, Perrone G (2015) Developing fragility curves and loss functions for masonry infill walls. Earthquake Structures 9(1):257–279. https://doi.org/10.12989/eas.2015.9.1.257
23. Szagri D, Szalay Z (2022) Theoretical fragility curves - A novel approach to assess heat vulnerability of residential buildings. Sustainable Cities Soc 83. https://doi.org/10.1016/J.SCS.2022.103969
24. Applied Techonology Council (2019) Performance Assessment Calculation Tool (PACT) - Calculation Tool. https://femap58.atcouncil.org/pact
25. Zhu M (2018) The OpenSeesPy Library — OpenSeesPy 3.5.1.3 documentation. https://openseespydoc.readthedocs.io/en/latest/
26. Ladybug Tools (2023) Ladybug Tools 1.7.26 — Honeybee. https://www.ladybug.tools/honeybee.html
27. US Department of Energy (2019) EnergyPlus Energy Simulation Software
28. European Facilities for Earthquake Hazard and Risk (EFEHR) (2021) EFEHR Web Platform - Hazard Spectra. http://hazard.efehr.org/en/hazard-data-access/hazard-spectra/
29. ASCE (2010) ASCE 7-10: Minimum Design Loads for Buildings and Other Structures
30. Ciurlanti J et al (2019) Feasibility Study of Low Damage Technology For HighRise Precast Concrete Buildings. Earthquake risk and engineering towards a resilient world
31. Hulley GC, Dousset B, Kahn BH (2020) Rising trends in heatwave metrics across Southern California. Earth's Future 8(7). https://doi.org/10.1029/2020EF001480
32. Flores-Larsen S, Bre F, Hongn M (2022) A performance-based method to detect and characterize heatwaves for building resilience analysis. Renewable Sustainable Energy Rev 167. https://doi.org/10.1016/J.RSER.2022.112795
33. Erlat E, Türkeş M, Güler H (2022) Analysis of long-term trends and variations in extreme high air temperatures in May over Turkey and a recordbreaking heatwave event of May 2020. Int J Climatol 42(16):9319–9343. https://doi.org/10.1002/joc.7821
34. Solcast (2016) Solcast API Toolkit. https://toolkit.solcast.com.au/historica
35. ASHRAE (2016) Standard 90.1 Appendix G 2013: Performance Rating Method. Tech. rep
36. Met Office (2022) UK Climate Change in action – The threshold temperatures. https://www.metoffice.gov.uk/about-us/press-office/news/weather-and-climate/2022/heatwave-threshold-changes
37. Klein T (2013) Integral Façade Construction Towards a new product architecture for curtain walls. Arch Built Environ